NONLINEAR INERTIAL COUPLING IN ASYMMETRIC BASE-ISOLATED STRUCTURES

Majid AMIN AFSHAR
Assistant Professor, Department of Civil Engineering, Imam Khomeini International University, Qazvin, Iran
mafshar@eng.ikiu.ac.ir

Sepehr AGHAEI POUR
MSc student, Department of Civil Engineering, Imam Khomeini International University, Qazvin, Iran
sepehr_aghaeipour@yahoo.com

Keywords: Structural Dynamics, Asymmetric, Base Isolator, Nonlinear Inertial, Coupling

ABSTRACT

It has been well proved that seismic base isolation systems, as passive tools of structural control, mitigate the intensity of damage caused by earthquakes. On the other hand, structures are often built in irregular plans, which lead to much more damage under earthquake motions. So, the present research dealt with the dynamic interaction of asymmetric base-isolated structures in a new point of view. The motion equations were presented in two coordinates: one fixed on the building base (inertial or global coordinate) and the other at the torsional isolation level (local coordinate), which led to linear and nonlinear forms of equations, respectively. Two types of structures were defined with different natural frequencies. Responses of both linear and nonlinear models for the two types of structures under harmonic effects were compared while analyzing time history and frequency. Some non-linear phenomena such as saturation and energy transfer between the modes in such structures were observed. Historical response peaks of linear and nonlinear models under real earthquake were compared in terms of various base torsional natural frequencies of the base isolation system in different directions. It can be inferred from the results of the analysis that nonlinear responses can be more critical than linear ones and design prescriptions should be adapted regarding nonlinear effects.

INTRODUCTION

Severe damage to buildings, as a result of earthquake, is caused by torsional motions due to irregularity. Observations have shown that earthquakes can cause more damage to asymmetric-plan structures than comparable symmetric-plan ones. Today, base isolation of buildings is a conventional approach to earthquake resistance. The prominent goal of this method was to reduce the displacement of the main structure by moving elastomeric bearings installed on the substructures. It has been demonstrated that the base isolation is the common method of damage reduction in asymmetric structures (Kelly and Naeim, 1999).

Many previous works have emphasized the linear model of isolated structures in the global coordinate system. Kilar and Koren (2009) determined the most appropriate distribution of isolators in the asymmetric plan; they observed that, when the center of mass was based on the center of distribution of the base isolation, the torsional effect was reduced in the isolation system. Seguín et al. (2008) studied the earthquake response of isolated structure with lateral-torsional correlation. The results showed that the UBC code did not have accurate estimation of the edge displacement under the static approximation; so, it required precise revision in the mentioned subject. Sharma and Jangid (2009), by utilizing the motion equations of the isolated structure, showed that high initial stiffness in the isolation system could create intense modes in the superstructure and lead to more displacement at the story level. The common point of such studies was in exploiting the dynamics of models because of lateral-torsional coupling in the global coordinate.

Several studies have also investigated the nonlinear dynamical behavior of structures. For instance, inclined cables carrying moving oscillators (Sofi, 2013) and inclined beam subjected to moving mass (Mamandi et al., 2010b, Mamandi et al., 2010a) have been studied in terms of local coordinate and nonlinear inertia as well as some corresponding nonlinear phenomena.

On the whole, most researchers in the field of structural engineering have paid less attention to the nonlinearity of inertia in conventional skeleton buildings. Even considering the smallest responses and excitations affected by the nonlinear terms in the governing equations of the nonlinear system is the substantial point which could lead to the unusual and strange phenomena. Saturation, jump, hysteretic cycle, etc. are nonlinear phenomena that are not observed in the linear models of mechanical systems (Nayfeh, 2000). So far, DOFs of structures have been defined on the direction of fixed axes of the global system in the asymmetric isolated structures. The result of this conventional approach leads to the motion equations of isolated structures in the linear form, while the axes representing the parameters of structural stiffness are not fixed and rotate by the angle of twisting floor. Hence the equations should be calculated based on these rotational axes. This novel approach in the definition of dynamical characteristics of structures leads to dramatic changes in the dynamic equation governing the torsional-lateral coupled behavior of the irregular isolated structure (nonlinear form). The main goal of this paper was to derive and compare the motion equations of the linear and nonlinear models of the one-way asymmetric isolated structure. Numerical analysis was carried out by defining two specific types of structures subjected to harmonic excitations. Historical response peaks of such models were compared in terms of various torsional natural frequencies of substructure in different directions. The paper was concluded with a brief discussion of the obtained results.

EQUATIONS OF MOTION

An isolated single story structure with one-way asymmetric plan was studied. Floor diaphragms of the superstructure and base isolation were assumed rigid in its own plane and plane frames ran in two orthogonal directions. The floor masses (i.e. m_s and m_b) were distributed uniformly at the floor levels. The resisting elements such as beams and columns provided elastic forces in the opposite direction of translational motions and proportional to their in-plane stiffness. Hence, the center of resistance coincided with the center of stiffness. Centers of mass and stiffness were denoted by $C.M_b$ and $C.R_b$ in the base isolation and $C.M_s$ and $C.R_s$ in the superstructure, respectively. $C.M_b$ and $C.M_s$ were situated along a line about the vertical axis Z. Due to the asymmetric distribution of stiffness only about Y axis, $C.R_b$ and $C.R_s$ were at distances e_{xb} and e_{xs} from the center of mass along X axis.

Earthquake excitations (r_g) entered the building under arrival angle β from X. Two coordinates were defined in this research. Global coordinate system (XYZ) was fixed on the building base (Chopra, 2007) and local ones ($x_b y_b z_b$) were fixed on the mass center of the base isolation system ($C.M_b$) which rotated at rotational angle θ_b (Fig. 1). Because of the larger amount of stiffness of the superstructure in comparison with that of the base isolation, structure rotation θ_s had a lower order than the base one θ_b. So, all the stiffness and damping were described in new directions of the substructures' floor edges.

The motions of the base isolation and superstructure floors were described by 6-DOFs in the directions of global coordinate axes, respectively: displacement in the X-direction, u_{Xb} and u_{Xs}, displacement in the Y-direction, u_{Yb} and u_{Ys}, and rotation of the floor about the vertical axis Z through the center of mass, $u_{\theta b}$ and $u_{\theta s}$. Such DOFs were also denoted by u_{xb}, u_{yb}, and $u_{\theta b}$ for the base isolation and u_{xs}, u_{ys}, and $u_{\theta s}$ for the superstructure along local coordinate axes.

Static and dynamic characteristics including stiffness (k_{xb}, k_{yb}, $k_{\theta Rb}$, k_{xs}, k_{ys} and $k_{\theta Rs}$) and damping (c_{xb}, c_{yb}, $c_{\theta b}$, c_{xs}, c_{ys} and $c_{\theta s}$) as well as the DOFs of the base isolation and superstructure were defined along the fixed axes of global coordinate. It means that these parameters were independent from the torsion of the base isolation floor (Fig. 1a). However, the axes representing structural stiffness and damping parameters were not fixed and rotated with the torsional angle of the base floor; in other words, these parameters could be better defined as local variables in the directions of rotary coordinate fixed on the mass center of the base isolation (Fig. 1b). In Fig. 1, initial position and relative motions of base isolation and superstructure diaphragm are denoted by pale, normal, and dark grey rectangles, respectively.

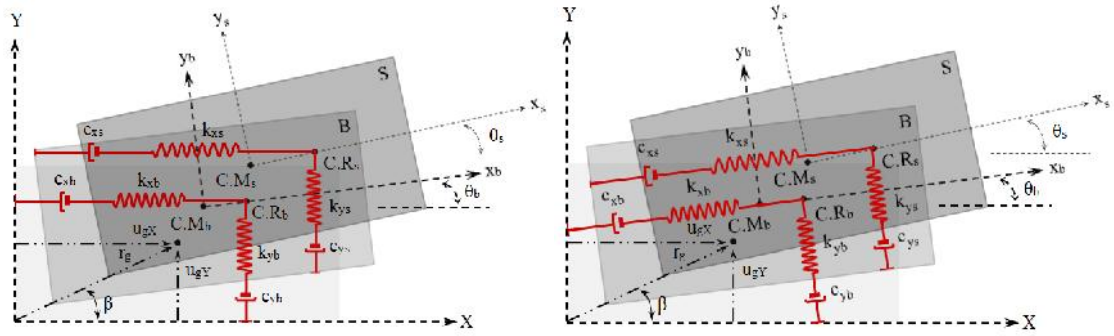

Figure 1. Global (XYZ) and local ($x_b y_b z_b$) coordinates and directions of static and dynamic characteristics of the base isolation and superstructure consisting of stiffness and damping in (a) linear and (b) nonlinear models

Lagrangian method was employed to achieve the equations of linear and nonlinear models (Amin Afshar and Amini, 2012, Amini and Amin Afshar, 2011). Motion equations of the isolated structure in the global and local coordinates were computed by Eq. (1).

$$F_{qi} = \frac{d}{dt}\left(\frac{\partial L}{\partial \dot{q}_i}\right) - \frac{\partial L}{\partial q_i} \tag{1}$$

in which q_i are the generalized coordinates of the 6-DOFs defined in either the global system (u_{Xb}, u_{Yb}, $u_{\theta b}$, u_{Xs}, u_{Ys}, and $u_{\theta s}$) or local one (u_{xb}, u_{yb}, $u_{\theta b}$, u_{xs}, u_{ys}, and $u_{\theta s}$), F_{qi} are external non-conservative forces such as excitation and damping forces, and L is the Lagrangian function defined as L=T–V, where T and V represent the kinetic and potential energies, respectively. First, the potential energy stored in resisting elements and total kinetic energy were calculated by Eqs. (2) and (3), respectively.

$$\begin{aligned} V = {} & \frac{1}{2}k_{xb}u_{xb}^2 + \frac{1}{2}k_{yb}\left(u_{yb} + e_{xb}u_{-b}\right)^2 + \frac{1}{2}k_{-Rb}u_{-b}^2 \\ & + \frac{1}{2}k_{xs}\left(u_{xs} - u_{xb}\right)^2 + \frac{1}{2}k_{ys}\left[\left(u_{ys} - u_{yb}\right) + e_{xs}\left(u_{-s} - u_{-b}\right)\right]^2 + \frac{1}{2}k_{-Rs}\left(u_{-s} - u_{-b}\right)^2 \end{aligned} \tag{2}$$

$$\begin{aligned} T = {} & \frac{1}{2}m_b\left(\frac{du_{Xb}}{dt}\right)^2 + \frac{1}{2}m_b\left(\frac{du_{Yb}}{dt}\right)^2 + \frac{1}{2}m_b r_b^2\left(\frac{du_{-b}}{dt}\right)^2 \\ & + \frac{1}{2}m_s\left(\frac{du_{Xs}}{dt}\right)^2 + \frac{1}{2}m_s\left(\frac{du_{Ys}}{dt}\right)^2 + \frac{1}{2}m_s r_s^2\left(\frac{du_{-s}}{dt}\right)^2 \end{aligned} \tag{3}$$

where r_b and r_s are the floor radii of the gyration of the base isolation and superstructure about the center of mass, respectively. The global variables were related to the local ones by rotating the local axes counter-clockwise at angle θ_b utilizing Eqs. (4) – (9).

$$u_{Xs} = u_{xs}^b \cos\bar{}_b - u_{ys}^b \sin\bar{}_b + u_{gX} \tag{4}$$

$$u_{Ys} = u_{xs}^b \sin\bar{}_b + u_{ys}^b \cos\bar{}_b + u_{gY} \tag{5}$$

$$u_{-s} = \bar{}_s \tag{6}$$

$$u_{Xb} = u_{xb}^b \cos\bar{}_b - u_{ys}^b \sin\bar{}_b + u_{gX} \tag{7}$$

$$u_{Yb} = u_{xb}^b \sin\bar{}_b + u_{yb}^b \cos\bar{}_b + u_{gY} \tag{8}$$

$$u_{-b} = \bar{}_b \tag{9}$$

Eqs. (2) and (3) were inserted in Eq. (1); afterwards, Eq. (1) was applied for each generalized coordinate of the global system. Motion equations of the linear model were thus obtained.

$$m_b\ddot{u}_{Xb}+\left(c_{xb}+c_{xs}\right)\dot{u}_{Xb}+\left(k_{xb}+k_{xs}\right)u_{Xb}-c_{xs}\dot{u}_{Xs}-k_{xs}u_{Xs}=-m_b\ddot{u}_{gX} \tag{10}$$

$$m_b\ddot{u}_{Yb}+\left(c_{yb}+c_{ys}\right)\dot{u}_{Yb}+\left(k_{yb}+k_{ys}\right)u_{Yb}+\left(e_{xb}c_{yb}+e_{xs}c_{ys}\right)\dot{u}_{-b}-c_{ys}\dot{u}_{Ys}-e_{xs}c_{ys}\dot{u}_{-s}+\left(e_{xb}k_{yb}+e_{xs}k_{ys}\right)u_{-b}-k_{ys}u_{Ys}-e_{xs}k_{ys}u_{-s}=-m_b\ddot{u}_{gY} \tag{11}$$

$$m_b r_b^2\ddot{u}_{-b}+\left(c_{-b}+c_{-s}\right)\dot{u}_{-b}+\left(k_{-Rb}+e^2{}_{xb}k_{yb}+k_{-Rs}+e^2{}_{xs}k_{ys}\right)u_{-b}+\left(e_{xb}c_{yb}+e_{xs}c_{ys}\right)\dot{u}_{Yb}-e_{xs}c_{ys}\dot{u}_{Ys}-c_{-s}\dot{u}_{-s}+\left(e_{xb}k_{yb}+e_{xs}k_{ys}\right)u_{Yb}-e_{xs}k_{ys}u_{Ys}-\left(k_{-Rs}+e^2{}_{xs}k_{ys}\right)u_{-s}=0 \tag{12}$$

$$m_s\ddot{u}_{Xs}+c_{xs}\dot{u}_{Xs}+k_{xs}u_{Xs}-c_{xs}\dot{u}_{Xb}-k_{xs}u_{Xb}=-m_s\ddot{u}_{gX} \tag{13}$$

$$m_s\ddot{u}_{Ys}+c_{ys}\dot{u}_{Ys}+k_{ys}u_{Ys}-c_{ys}\dot{u}_{Yb}-e_{xs}c_{ys}\dot{u}_{-b}+e_{xs}c_{ys}\dot{u}_{-s}-k_{ys}u_{Yb}-e_{xs}k_{ys}u_{-b}+e_{xs}k_{ys}u_{-s}=-m_s\ddot{u}_{gY} \tag{14}$$

$$m_s r_s^2\ddot{u}_{-s}+c_{-s}\dot{u}_{-s}+\left(k_{-Rs}+e_{xs}^2k_{ys}\right)u_{-s}-e_{xs}c_{ys}\dot{u}_{Yb}-c_{-s}\dot{u}_{-b}+e_{xs}c_{ys}\dot{u}_{Ys}-e_{xs}k_{ys}u_{Yb}-\left(k_{-Rs}+e_{xs}^2k_{ys}\right)u_{-b}+e_{xs}k_{ys}u_{Ys}=0 \tag{15}$$

Eqs. (4) - (9) were inserted in Eq. (3); then, Eq. (1) was applied to each DOF of the local system. Motion equations of nonlinear model of isolated structure were also obtained.

$$m_b\ddot{u}_{xb}^b+\left(c_{xb}+c_{xs}\right)\dot{u}_{xb}^b+\left(k_{xb}+k_{xs}\right)u_{xb}^b-c_{xs}\dot{u}_{xs}^b-k_{xs}u_{xs}^b=-m_b\left(-2\dot{u}_{yb}^b\dot{u}_{-b}-u_{yb}^b\ddot{u}_{-b}-u_{xb}^bu_{-b}^2+\ddot{u}_{gX}\cos^{-}{}_b+\ddot{u}_{gY}\sin^{-}{}_b\right) \tag{16}$$

$$m_b\ddot{u}_{yb}^b+\left(c_{yb}+c_{ys}\right)\dot{u}_{yb}^b+\left(k_{yb}+k_{ys}\right)u_{yb}^b+\left(e_{xb}c_{yb}+e_{xs}c_{ys}\right)\dot{u}_{-b}-c_{ys}\dot{u}_{ys}^b-e_{xs}c_{ys}\dot{u}_{-s}+\left(e_{xb}k_{yb}+e_{xs}k_{ys}\right)u_{-b}-k_{ys}u_{ys}^b-e_{xs}k_{ys}u_{-s}=-m_b\left(2\dot{u}_{xb}^b\dot{u}_{-b}+u_{xb}^b\ddot{u}_{-b}-u_{yb}^b\dot{u}_{-b}^2-\ddot{u}_{gX}\sin^{-}{}_b+\ddot{u}_{gY}\cos^{-}{}_b\right) \tag{17}$$

$$m_b r_b^2\ddot{u}_{-b}+\left(c_{-b}+c_{-s}\right)\dot{u}_{-b}+\left(k_{-Rb}+e^2{}_{xb}k_{yb}+k_{-Rs}+e^2{}_{xs}k_{ys}\right)u_{-b}+\left(e_{xb}c_{yb}+e_{xs}c_{ys}\right)\dot{u}_{yb}^b-e_{xs}c_{ys}\dot{u}_{ys}^b-c_{-s}\dot{u}_{-s}+\left(e_{xb}k_{yb}+e_{xs}k_{ys}\right)u_{yb}^b-e_{xs}k_{ys}u_{ys}^b-\left(k_{-Rs}+e^2{}_{xs}k_{ys}\right)u_{-s}=0 \tag{18}$$

$$m_s\ddot{u}_{xs}^b+c_{xs}\dot{u}_{xs}^b+k_{xs}u_{xs}^b-c_{xs}\dot{u}_{xb}^b-k_{xs}u_{xb}^b=-m_s\left(-2\dot{u}_{ys}^b\dot{u}_{-b}-u_{ys}^b\ddot{u}_{-b}-u_{xs}^bu_{-b}^2+\ddot{u}_{gX}\cos^{-}{}_b+\ddot{u}_{gY}\sin^{-}{}_b\right) \tag{19}$$

$$m_s\ddot{u}_{ys}^b+c_{ys}\dot{u}_{ys}^b+k_{ys}u_{ys}^b-c_{ys}\dot{u}_{yb}^b-e_{xs}c_{ys}\dot{u}_{-b}+e_{xs}c_{ys}\dot{u}_{-s}-k_{ys}u_{yb}^b-e_{xs}k_{ys}u_{-b}+e_{xs}k_{ys}u_{-s}=-m_s\left(2\dot{u}_{xs}^b\dot{u}_{-b}^2+u_{xs}^b\ddot{u}_{-b}-u_{ys}^b\dot{u}_{-b}^2-\ddot{u}_{gX}\sin^{-}{}_b+\ddot{u}_{gY}\cos^{-}{}_b\right) \tag{20}$$

$$m_s r_s^2\ddot{u}_{-s}+c_{-s}\dot{u}_{-s}+\left(k_{-Rs}+e^2{}_{xs}k_{ys}\right)u_{-s}-e_{xs}c_{ys}\dot{u}_{yb}^b-c_{-s}\dot{u}_{-b}+e_{xs}c_{ys}\dot{u}_{ys}^b-e_{xs}k_{ys}u_{yb}^b-\left(k_{-Rs}+e^2{}_{xs}k_{ys}\right)u_{-b}+e_{xs}k_{ys}u_{ys}^b=0 \tag{21}$$

in which c_{xb}, c_{yb}, $c_{\theta b}$, c_{xs}, c_{ys}, and $c_{\theta s}$ are damping coefficients of the base isolation and superstructure and $\ddot{u}_{gX}$ and $\ddot{u}_{gY}$ are translational ground accelerations in the X and Y directions. In Eqs. (16) - (21), all the accelerations, velocities, and displacements were defined in the directions of local coordinate axes; but, such variables included in Eqs. (10) - (15) were defined in the direction of global coordinate axes. The substantial difference between two models was in terms of the right side of their equations where nonlinear inertial terms can be observed in the nonlinear model. Obviously, in numerical analysis, nonlinear model responses

calculated by Eqs. (16) - (21) should be transferred to global coordinate by the corresponding rotation matrix and then compared with that of the linear ones.

NUMERICAL ANALYSIS

To evaluate performance of the linear and nonlinear models, numerical analysis is done by harmonic excitations and Kobe 1995 earthquake. The natural frequency of symmetric direction of the superstructure (ω_{xs}) related to the one story building was considered equal to 20π (rad/s). Other frequencies of the superstructure and base isolation were assessed by ω_{xs} as follows:

$$\Omega_{xb}=\frac{\mu_{xb}}{\mu_{xs}},\Omega_{\bar{}b}=\frac{\mu_{\bar{}b}}{\mu_{xs}},\Omega_{yb}=\frac{\mu_{yb}}{\mu_{xs}},\Omega_{xs}=\frac{\mu_{xs}}{\mu_{xs}},\Omega_{\bar{}s}=\frac{\mu_{\bar{}s}}{\mu_{xs}},\Omega_{ys}=\frac{\mu_{ys}}{\mu_{xs}} \tag{22}$$

in which Ω_{xb}, Ω_{yb}, Ω_{xs}, and Ω_{ys} are the ratio of the translational uncoupled frequencies and $\Omega_{\theta b}$ and $\Omega_{\theta s}$ are the ratio of the rotational ones. Obviously, the stiffness of an isolator in X and Y directions are identical, which leads to $\Omega_{xb}=\Omega_{yb}$.

Two structures were defined to study linear and nonlinear responses. The differences were just observed in their $\Omega_{\theta b}$ and e_{xb}/r. The other structure properties were equivalent to each other (Table 1). The ratios were selected so that at least one of the torsional-lateral correlated frequency ratios of the structure type 2 could be equal to 0.5; however, this feature was not provided in the first one (Table 1).

Table 1. Properties of two types of structures

Type No.	Ω_{xb}	$\Omega_{\theta b}$	Ω_{yb}	Ω_{xs}	$\Omega_{\theta s}$	Ω_{ys}	e_{xb}/r	e_{xs}/r	m_s/m_b	Ω_1	Ω_2
1	0.1	0.15	0.1	1	0.7	0.5	0.6	0.2	5	0.863	1.552
2	0.1	0.105	0.1	1	0.7	0.5	0.8	0.2	5	0.500	1.334

The responses were employed for 6-DOFs of motion of the base isolation and superstructure, i.e. u_{xb}, u_{yb}, $u_{\theta b}$, u_{xs}, u_{ys}, and $u_{\theta s}$, in time history and frequency content analyses. Frequency domain responses were obtained using a fast Fourier transform (FFT) to determine the contribution of the structural modes in the absorption of the excitation energy. The frequencies corresponding to the peak points in the frequency contents denotes the natural frequencies of the dominant modes of structure and peak points denotes the rate of energy absorption by natural modes or excitation frequencies.

Due to the larger stiffness of the superstructure to the base, the superstructure acted as a rigid body on the soft base isolation affected by earthquake. Two cases were defined between torsional-lateral correlated frequency and symmetric one. In the first manner, the ratio of the first asymmetric to symmetric frequency was assumed to equal 0.5 (Ω_1=0.5) called proportional resonance (Eq. (23)); in the second one, Ω_2-Ω_1=1 was called subtractive combinatorial resonance (Eq. (24)).

$$12\Omega_{\bar{}b}^2-16e_{xb}^2\Omega_{yb}^2-3\Omega_{yb}^2=0 \tag{23}$$

$$(\Omega_{\bar{}Rb}-\Omega_{yb})^2+e_{xb}^2\Omega_{yb}^2=1 \tag{24}$$

The resonances were employed during comparing maximum historical responses of the rigid superstructure with the range of base isolation torsional frequency under Kobe earthquake; therefore, the superstructure properties (Ω_{xs}, Ω_{ys}, $\Omega_{\theta s}$, and e_{xs}/r) were assumed constant as in Table 1, whereas the base isolation properties were obtained based on Eqs. (23) and (24).

RESPONSE TO HARMONIC EXCITATIONS

Excitation force vector or ground acceleration is defined as the harmonic force equal to $A\omega^2\sin(\omega t)$, where ω is excitation frequency and A is ratio of ground acceleration amplitude to radius of gyration. In further studies, rather than excitation frequency ω, dimensionless parameter Ω equal to frequency ratio ω/ω_{x1} has been used, where ω_{x1} is natural frequency of the first mode of the symmetric direction, excitation amplitude is 0.05, and entry angle and structure damping ratio are considered of 60° to the X axis and 2%,

respectively.

Initially, harmonic excitation with excitation frequency equal to the first mode of symmetric frequency (Ω=1) was exerted on structure 1 (Fig. 2). It can be observed that responses of both linear and nonlinear models were exactly identical in the time and frequency response. The peak values of the response in the directions of X, Y, and θ occurred at the first mode of symmetric frequency.

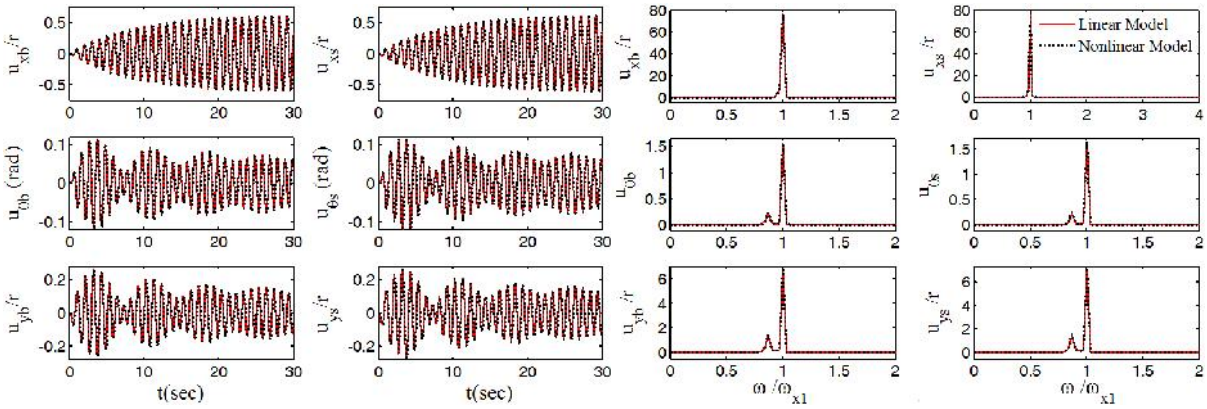

Figure 2. Time history and frequency content of structure type 1 under frequency ratio Ω=1

Time history and frequency content of the structure type 2 were investigated under first mode of symmetric frequency (Fig. 3) and first torsional-lateral correlated frequency (Fig. 4). In the time history, the nonlinear DOFs acted differently from that of the linear one. In Fig. 3, both linear and nonlinear models had a peak in the first mode of symmetric frequency response of X displacement although the nonlinear values were too smaller. In Y and θ displacements, the response peaks were just observed at the first asymmetric frequency in nonlinear model. The frequency responses of X displacement in Fig. 4 showed that the nonlinear model only had a response peak in the first mode of symmetric frequency, whereas in Y and θ displacements, each model had a peak at the first torsional-lateral frequency and the linear one showed a greater value. It can be inferred that the more the increased amplitude of harmonic excitations, the larger the difference between responses of two models would be. Studying base isolation's DOFs represented similar results to those of the superstructure ones.

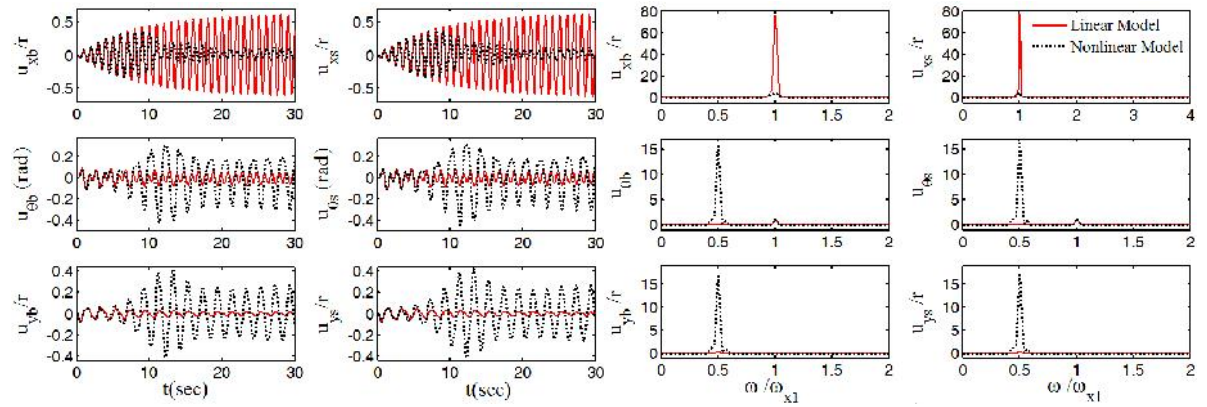

Figure 3. Time history and frequency content of structure type 2 under frequency ratio Ω=1

The nonlinear model in the initial time indicated the same performance as the linear one; i.e. the DOFs of symmetric direction behaved independently from other DOFs of the structure until the specific time, when the symmetric responses of the structure absorbed a certain amount of excitation energy; from that moment called saturation moment, the performance of the two models became different. In other words, when X displacement responses reached the specific energy, it was saturated; afterwards, all the responses of the nonlinear model in three directions acted as coupled variables and the energy transferred from dominant response in symmetric direction with high natural frequency (Ω=1) to dominant response in lateral and torsional directions with low natural frequency ($\Omega=\Omega_1$); so, the amplitudes of the X displacements were reduced, while the amplitudes of Y and θ directions were increased compared with that of the linear model.

This behavior of the nonlinear model was called saturation phenomenon and can be observed in Fig. 3.

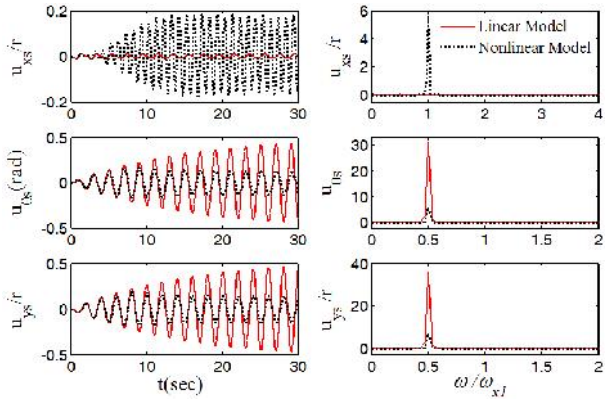

Figure 4. Time history and frequency content of structure type 2 under frequency ratio $\Omega=\Omega_1$

However, saturation phenomenon did not occur in Fig. 4, so that indication of nonlinear behavior could not have a start point. Hence, the energy transferred from low natural frequency ($\Omega=\Omega_1$) to high natural frequency ($\Omega=1$) at the very beginning of the oscillation.

VARIATIONS OF BASE ISOLATION TORSIONAL FREQUENCY

As was mentioned, base isolation frequencies in the symmetric and asymmetric directions were identical to each other ($\Omega_{xb}=\Omega_{yb}=0.1$). To observe soft, normal, and hard situations of the base isolation torsion to the first mode frequency of symmetric frequency, a range of $\omega_{\theta b}/\omega_{x1}$ between 0.6 and 1.4 was assumed. The eccentric ratios of base isolation were provided using Eqs. (23) and (24) under proportional and subtractive resonances, respectively (Fig. 5). The results were just obtained under Kobe earthquake for the superstructure although the base isolation DOFs yielded the same ones.

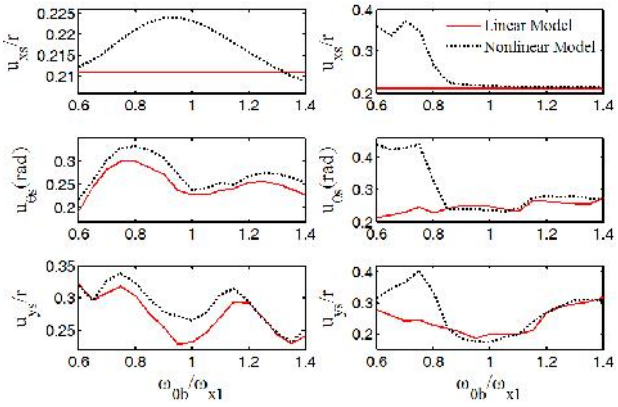

(a) (b)

Figure 5. Maximum responses for the range of $\omega_{\theta b}/\omega_{x1}$ under e_{xb}/r corresponding to (a) proportional and (b) subtractive resonance

The X displacements of linear responses were always constant, while the nonlinear ones indicated greater values. Stability of linear responses in the symmetric direction was because of the independence of linear equation from torsional-lateral properties such as $\omega_{\theta b}$ and e_{xb}, while the DOFs of nonlinear model were correlated due to the nonlinear inertia terms, which caused the energy transfer. In Y and θ displacements, the nonlinear responses were almost greater than those of the linear ones under the proportional resonance as well as the soft situation under subtractive resonance. By approaching two model responses in the larger $\omega_{\theta b}/\omega_{x1}$, it can be inferred that effect of nonlinear inertia was reduced, while $\omega_{\theta b}/\omega_{x1}$ increased. The nonlinear model was more critical than the linear one; so, the nonlinear inertia effects should be considered in the design of structures.

CONCLUSIONS

Movement of asymmetric base-isolated structure was described by 6 DOFs. The motion equations of two linear and nonlinear models were represented in terms of two coordinate systems defined for such degrees of freedom. Time history and frequency responses of two structures were studied under harmonic excitations. Maximum historical responses of the linear and nonlinear models were compared with the variations of $\omega_{\theta b}$. The results of observation is summarized as follows:

- Time history and frequency content of two linear and nonlinear models were in exact coincidence in the structure type 1. This coincidence was independent from the amplitude and frequency of excitation as well as the arrival angle of excitation under harmonic forces.
- In the saturation phenomenon, the energy absorbed by the response of one direction was saturated at the specific moment; after that time, the rest of energy, which had the harmonic response with greater natural frequency, was transferred to the other direction with lower natural frequency. In the energy transfer phenomenon similar to the saturation phenomenon, transfer of energy occurred, with the difference that the transition began from the first moments of excitation and did not have any specific strating point. This nonlinear behavior can be observed in the structure type 2.
- Investigating of the variations of base isolation torsion showed that the nonlinear model was more critical. The nonlinear model should be employed to provide design criteria.
- The difference between the responses of the linear and nonlinear models was because of the existence of nonlinear inertial terms in the nonlinear model which caused the DOFs of the symmetric and asymmetric directions behave dependently.

REFERENCES

Amin Afshar M and Amini F (2012) Non-linear dynamics of asymmetric structures under 2: 2: 1 resonance, *International Journal of Non-Linear Mechanics*, 47(7): 823-835

Amini F and Amin Afshar M (2011) Saturation in asymmetric structures under internal resonance, *Acta mechanica*, 221(3-4): 353-368

Chopra AK (2007) Dynamics of structures: Theory and Applications to earthquake engineering, Prentice Hall, New Jersey

Kelly J M and Naeim F (1999) Design of seismic isolated structures: From theory to practice, John Wiley and Sons, Nueva York

Kilar V and Koren D (2009) Seismic behaviour of asymmetric base isolated structures with various distributions of isolators, *Engineering structures*, 31(4): 910-921

Mamandi A, Kargarnovin MH and Farsi S (2010a) An investigation on effects of traveling mass with variable velocity on nonlinear dynamic response of an inclined Timoshenko beam with different boundary conditions, *International Journal of Mechanical Sciences*, 52(12)**:** 1694-1708

Mamandi A, Kargarnovin MH and Younesian D (2010b) nonlinear dynamics of an inclined beam subjected to a moving load, *Nonlinear Dynamics*, 60(3)**:** 277-293

Nayfeh A (2000) Nonlinear Interactions: Analytical, Computational, and Experimental Methods, John Wiley and Sons, New York

Seguín C E, De La Llera J C and Almazán JL (2008) Base–structure interaction of linearly isolated structures with lateral–torsional coupling, *Engineering Structures*, 30(1)**:** 110-125

Sharma A and Jangid R (2009) Behaviour of Base-Isolated Structures with High Initial Isolator Stiffness, *International Journal of Applied Science, Engineering and Technology*, 5(3): 199-204

SOFI A (2013) nonlinear in-plane vibrations of inclined cables carrying moving oscillators, *Journal of Sound and Vibration*, 332(7)**:** 1712-1724